

Article

# An Effective Approach towards the Immobilization of PtSn Nanoparticles on Noncovalent Modified Multi-Walled Carbon Nanotubes for Ethanol Electrooxidation

Xi Geng <sup>†</sup>, Yinjie Cen <sup>†</sup>, Richard D. Sisson and Jianyu Liang <sup>\*</sup>

Department of Mechanical Engineering, Worcester Polytechnic Institute, 100 Institute Road, Worcester, MA 01609, USA; xigeng@wpi.edu (X.G.); ycen@wpi.edu (Y.C.); Sisson@wpi.edu (R.D.S.)

\* Correspondence: jianyul@wpi.edu; Tel.: +1-508-831-6649; Fax: +1-508-831-5178

† These authors contributed equally to this work.

Academic Editor: Izumi Taniguchi

Received: 21 December 2015; Accepted: 29 February 2016; Published: 4 March 2016

**Abstract:** In this article, we describe an effective method to tether Pt and PtSn nanoparticles (NPs) on polyelectrolyte modified multi-walled carbon nanotubes (MWCNTs) for ethanol electrooxidation. By using a polymer wrapping technique, positively charged polyethyleneimine (PEI) was attached onto carbon nanotubes (CNTs) to provide preferential linking sites for metal precursors. Well-dispersed Pt and PtSn nanocrystals (2–5 nm) were subsequently decorated on PEI-functionalized MWCNTs through the polyol reduction method. The successful non-covalent modification of MWCNTs was confirmed by Fourier transform infrared spectroscopy (FTIR) and Zeta potential measurements. Energy dispersive X-ray (EDX) spectrum indicates approximately 20 wt % Pt loading and a desirable Pt:Sn atomic ratio of 1:1. Electrochemical analysis demonstrated that the as-synthesized PtSn/PEI-MWCNTs nanocomposite exhibited improved catalytic activity and higher poison tolerance for ethanol oxidation as compared to Pt/PEI-MWCNTs and commercial Pt/XC-72 catalysts. The enhanced electrochemical performance may be attributed to the uniform dispersion of NPs as well as the mitigating of CO self-poisoning effect by the alloying of Sn element. This modification and synthetic strategy will be studied further to develop a diversity of carbon supported Pt-based hybrid nanomaterials for electrocatalysis.

**Keywords:** polyethyleneimine (PEI); PtSn nanoparticles (NPs); multi-walled carbon nanotubes (MWCNTs); ethanol oxidation

## 1. Introduction

Direct ethanol fuel cells (DEFCs) are attracting research interest as an alternative power source for vehicles and portable electronic devices, because of their easy storage, high energy density, low toxicity, and abundant availability from biomass [1–5]. To date, carbon supported platinum (Pt) is the most commonly used electrocatalyst for ethanol oxidation [6]. However, the high cost and scarcity of Pt still hinder the commercialization of DEFCs [3]. It is well recognized that the catalytic activity and stability of electrocatalysts are strongly dependent on the particle size and dispersion of the noble metal on the carbon support. In the pursuit of improving Pt utilization, a variety of nanostructured carbon materials including carbon nanotubes (CNTs) [3,7–10], carbon nano fibers (CNFs) [11], carbon aerogel [12], and mesoporous carbon [13] have been investigated as potential catalyst supports.

Among these novel carbon materials, CNTs have intriguing features such as large active surface area, excellent electronic conductivity and high chemical stability, hence they are considered to be one of the promising candidates for Pt nanoparticles (NPs) support [7–10,14]. Since the pristine CNTs

are chemically inert and hydrophobic, a majority of the research has been dedicated to modifying their surface in order to promote better dispersion of Pt NPs. Recently, functionalization of carbon nanomaterials including nanocages [15], nanowires [16] and nanoclusters [17] through non-covalent attachment of polyelectrolyte has been developed to facilitate the growth of Pt NPs with well-defined shape and tunable size. As a versatile strategy, polyelectrolyte modification not only preserves the intrinsic structure of CNTs, but also achieves the tailored properties of the nanocomposites [18]. For example, highly-dispersed Pt NPs were deposited on the sidewalls of positively charged poly (diallyldimethylammonium chloride) coated CNTs with high density [19,20]. The amino-rich cationic Polyethyleneimine (PEI) has also been explored for the size-controlled synthesis of Pt NPs on CNTs [21–23], and as a stabilizing agent of Pt nanodendrites synthesis [24].

In addition to the high cost issue, another major challenge that hinders the commercialization of DEFCs, is the self-poisoning of Pt by intermediate species like CO. The CO-like intermediate products strongly adsorb on Pt active particles and decrease (poison) the catalytic activity of Pt during ethanol oxidation reaction (EOR) process. OH species react with CO-like intermediate products and free the Pt active particles [25,26]. Previous work on bimetallic catalyst systems demonstrated that the incorporation of a second metal, Sn in particular, could significantly mitigate the CO poisoning effect by generating oxygen-containing species, such as OH species, for the oxidative removal of CO-like species from adjacent Pt active sites, which is the so-called bifunctional mechanism [2,27,28]. In the past few years, several pathways have been explored to disperse PtSn NPs onto CNTs. Chen, *et al.* [29] demonstrated a microwave-assisted method to obtain a mesoporous open-ended structure. The Pechini method was also applied to acquire PtSn alloy ranging from 2 nm to 5 nm at 90 °C [30]. Trimetallic catalysts PtSnM (M = Ni, Co, Rh, Pd) had also been synthesized by Bönnemann method [31].

Zhou, *et al.* [32,33] found the catalytic performance of PtSn/C could be optimized by tuning the Pt:Sn molar ratio in a range from 1:1 to 2:1, which is similar to the results demonstrated by Spinacé, *et al.* [34] and Tsiakaras [35]. Lee, *et al.* [36] also presented a core-shell morphology via  $\gamma$ -irradiation method with 15 nm Pt core and 10 nm Sn shell.

Given the apparent benefit of bimetallic PtSn on carbon nanostructures as the catalyst support, controlled synthesis of PtSn NP with tunable loading level on CNTs is highly desirable. Report on using PEI functionalized CNTs to anchor bimetallic PtSn NP is lacking. With the goal of designing a high-performance catalyst with enhanced Pt utilization and good CO tolerance, we are presenting an efficient synthetic route to anchor bimetallic PtSn electrocatalyst on PEI functionalized CNTs. Figure 1 illustrates the scheme of the noncovalent surface modification of MWCNTs and the subsequent immobilization of PtSn NPs. According to transmission electron microscope (TEM) and scanning electron microscope (SEM) observations, Pt and bimetallic PtSn nanocrystals were uniformly decorated on PEI-functionalized MWCNTs. The composition, crystalline structure and electrochemical properties of the hybrid materials were investigated by energy dispersive X-ray (EDX), X-ray diffraction (XRD), cyclic voltammetry and chronoamperometry.

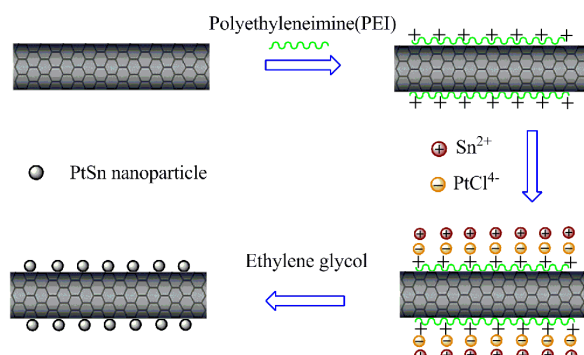


**Figure 1.** Schematic illustration showing the synthesis of PtSn electrocatalyst supported on polyethyleneimine-functionalized multi-walled carbon nanotubes (PEI-MWCNTs).

## 2. Experimental Section

### 2.1. Materials

Multi-walled carbon nanotubes (MWCNTs, 95% purity, diameter = 30–60 nm) were obtained from Helix Material Solutions, Inc. (Richardson, TX, USA). Potassium tetrachloroplatinate ( $K_2PtCl_4$ , 98%), Tin (II) chloride dihydrate ( $SnCl_2 \cdot 2H_2O$ , 98%), Nafion solution (5 wt % in ethanol), ethylene glycol (EG, 99%), and ethanol (99%) were purchased from Sigma-Aldrich (St. Louis, MO, USA). Polyethyleneimine (PEI 50 wt % in water,  $M_w = 60,000$ ), and sulfuric acid (98 wt %) were obtained from Alfa Aesar (Haverhill, MA, USA). Pt/XC-72 electrocatalyst with 20 wt % metal loading was purchased from E-TEK (Somerset, NJ, USA). All the chemicals were used as received without further purification. Ultrapure Milli-Q water (resistivity > 18.2  $M\Omega \cdot cm$ ) was exclusively used for making aqueous solutions and rinsing procedures.

### 2.2. Functionalization of Multi-Walled Carbon Nanotubes with Polyethyleneimine

Non-covalent functionalization of MWCNTs by PEI was carried out through a procedure modified from a prior publication [21]. Briefly, 100 mg of MWCNTs was dispersed into 200 mL 1 wt % PEI aqueous solution, followed by ultra-sonication for 3 h, and magnetic stirring for 12 h. The PEI-MWCNTs suspension was then filtered and rinsed to remove the excess PEI.

### 2.3. Synthesis of PEI-MWCNTs Supported Pt and PtSn Electrocatalysts

PtSn/PEI-MWCNTs nanocomposites were prepared by using a polyol reduction method described as follows: 100 mg PEI-CNTs was first suspended in an EG solution in an ultrasonic bath. An EG solution of  $K_2PtCl_4$  and  $SnCl_2$  with an atomic ratio of Pt:Sn = 1:1 was added dropwise under vigorous agitation to achieve the nominal Pt loading of 20 wt %. The metal precursors were reduced by refluxing the mixture at elevated temperatures of up to 140 °C for 3 h. A flow of ultra-high purity nitrogen was introduced to the reaction system to remove the gaseous organic byproducts. After centrifugation, washing by DI water and ethanol for three times each, and drying at 70 °C overnight, the PtSn/PEI-MWCNTs catalyst was obtained. For comparison purpose, the Pt/PEI-MWCNTs nanocomposite was also prepared in a similar manner, but in the absence of  $SnCl_2$ .

### 2.4. Physicochemical Characterization

Zeta potential measurements were performed on a Zetasizer Nano ZS90 (Marvern, Worcestershire, UK). Fourier transform infrared spectroscopy (FTIR) spectra were acquired using Vettex70 spectrometer (Bruker Optics, Billerica, MA, USA) to confirm the functionalization of MWCNTs by PEI. The morphology of the PtSn/MWCNTs nanocomposite was studied by a JEOL 7000F SEM and 100CX TEM (JEOL, Peabody, MA, USA). The average composition of the nanocomposites was evaluated using EDX. The XRD patterns of the samples were recorded using a Geigerflex X-ray diffractometer (Rigaku, Woodlands, Texas, USA) with Cu K $\alpha$  radiation.

### 2.5. Electrochemical Analysis

Electrochemical measurements were carried out on a BASi 100B electrochemical analyzer (BASi, West Lafayette, IN, USA) using conventional three-electrode cell. A glassy carbon electrode (GCE) (3 mm in diameter) was used as the working electrode, on which a thin layer of Nafion-impregnated catalyst with a fixed loading of 2 mg/cm<sup>2</sup> was applied. A platinum wire served as the counter electrode and an Ag/AgCl electrode was used as the reference electrode. The electrochemical active surface area (ECSA) was calculated from the hydrogen desorption region of the voltammetric curve in 0.5 M H<sub>2</sub>SO<sub>4</sub> solution. The electrocatalytic activity for ethanol oxidation was characterized by cyclic voltammetry (CV) in 0.5 M H<sub>2</sub>SO<sub>4</sub> solution containing 1 M C<sub>2</sub>H<sub>5</sub>OH. In order to evaluate the stability of the catalysts, chronoamperograms were also recorded at 0.6 V for 600 s. The electrolyte solution was

deaerated with ultra-high purity N<sub>2</sub> prior to the measurement, and all the experiments were conducted at room temperature.

### 3. Results and Discussion

#### 3.1. Zeta Potential Measurement of PEI-MWCNTs Nanocomposite

Zeta potentials as a function of pH for pristine and PEI-coated MWCNTs are presented in Figure 2. The sample of pristine MWCNTs is found to have a low initial isoelectric point ( $\text{pH}_{\text{IEP}}$ ) at 4.9. After treatment with PEI, the  $\text{pH}_{\text{IEP}}$  positively shifted to a more basic value at 8.1, indicating that the cationic PEI polymer chains are noncovalently attached onto the MWCNTs [37]. Since PEI has been widely reported to form complexes with various metal compound, such as K<sub>2</sub>PdCl<sub>4</sub>, K<sub>2</sub>PtCl<sub>4</sub> [21], AgNO<sub>3</sub> [38], and CuCl<sub>2</sub> [39], it is assumed that the positively charged amine groups of PEI may act as anchor sites for the negatively charged PtCl<sub>4</sub><sup>2-</sup> anions, which attract Sn<sup>2+</sup> cations through electrostatic forces. In-situ reduction of these metal precursors will favor the uniform assembly of Pt-based NPs on the surface of the PEI modified MWCNTs [32].

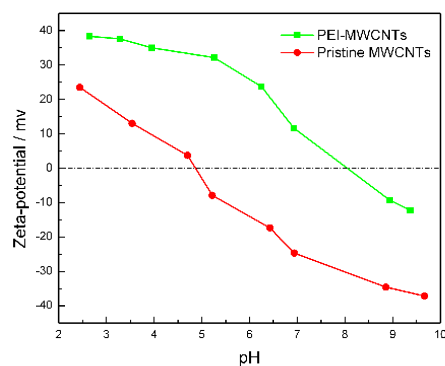


**Figure 2.** Zeta potential as a function of pH for pristine MWCNTs and PEI-MWCNTs.

#### 3.2. Fourier Transform Infrared Spectroscopy Spectra of Polyethyleneimine-Functionalized Multi-Walled Carbon Nanotubes

The FTIR spectra of pristine MWCNTs and PEI-MWCNTs are shown in Figure 3. There are three anticipated weak peaks at 1225 cm<sup>-1</sup>, 1578 cm<sup>-1</sup> and 1630 cm<sup>-1</sup> (marked by black asterisks) on the FTIR spectrum of pristine MWCNTs confirming the graphite structure of pristine MWCNTs [40]. The relatively sharp adsorption peak at 1637 cm<sup>-1</sup> (marked by red asterisks) on the FTIR spectrum of PEI-MWCNTs can be assigned to the bending vibration of N–H [37,40,41] and supports the conclusion of successful functionalization of MWCNTs with PEI. The FTIR and Zeta potential measurement results together verify the successful noncovalent modification of MWCNTs with PEI.

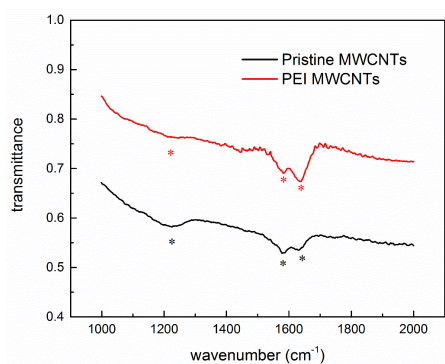


**Figure 3.** Fourier transform infrared spectroscopy (FTIR) spectra of pristine MWCNTs and PEI-MWCNTs.

### 3.3. Morphology and Composition of the As-Prepared Catalysts

TEM images and particle size distribution histograms of various electrocatalysts are shown in Figure 4. The severe agglomeration of Pt particles on XC-72 has been observed (Figure 4a) and made the characterization of particle size distribution rather difficult. In the case of Pt/PEI-MWCNTs and PtSn/PEI-MWCNT, Pt and bimetallic PtSn NPs are homogeneously deposited on the walls of PEI-MWCNTs (Figure 4b,d). As most of the particles are spherical without agglomeration, the mean particle size is estimated to be 2.9 nm for the former and 4.0 nm for the latter using the Gaussian fit (Figure 4c,e). The presence of PEI coating on MWCNTs probably contributed to obtaining relatively small particle sizes, with narrow distributions. The positively charged PEI molecules provide abundant adsorption sites for metal precursors, and may also serve as a stabilizing reagent to isolate the adjacent nanocrystals from agglomeration [42,43].

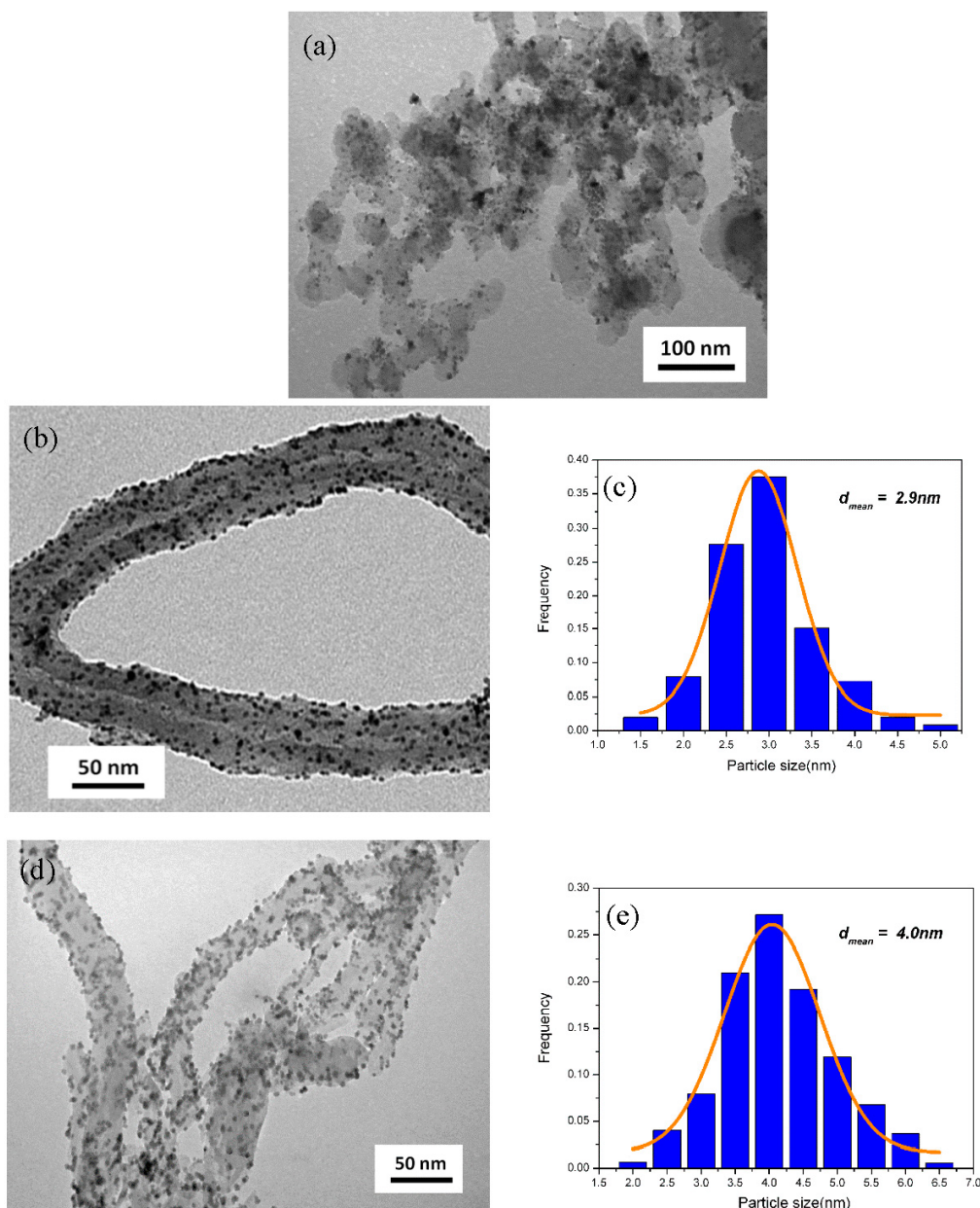


**Figure 4.** Transmission electron microscope (TEM) images and the corresponding particle size distribution of (a) Pt/XC-72; (b,c) Pt/PEI-MWCNTs; and (d,e) PtSn/PEI-MWCNTs.

As depicted in Figure 5, the coverage of Pt and PtSn NPs on PEI-MWCNTs is clearly shown through SEM and EDX. According to EDX analysis (Figure 5d,f), 20.3 wt % and 21.4 wt % Pt loading was obtained for Pt/PEI-MWCNTs and PtSn/PEI-MWCNTs, respectively. The average composition of PtSn/PEI-MWCNTs contains a Pt:Sn atomic ratio of 46:54. Those experimental data is very close to our targeted Pt loading of 20 wt % and initial feeding ratio 1:1, implying that the metal precursors have been reduced and deposited on the surface of modified MWCNTs as desired.

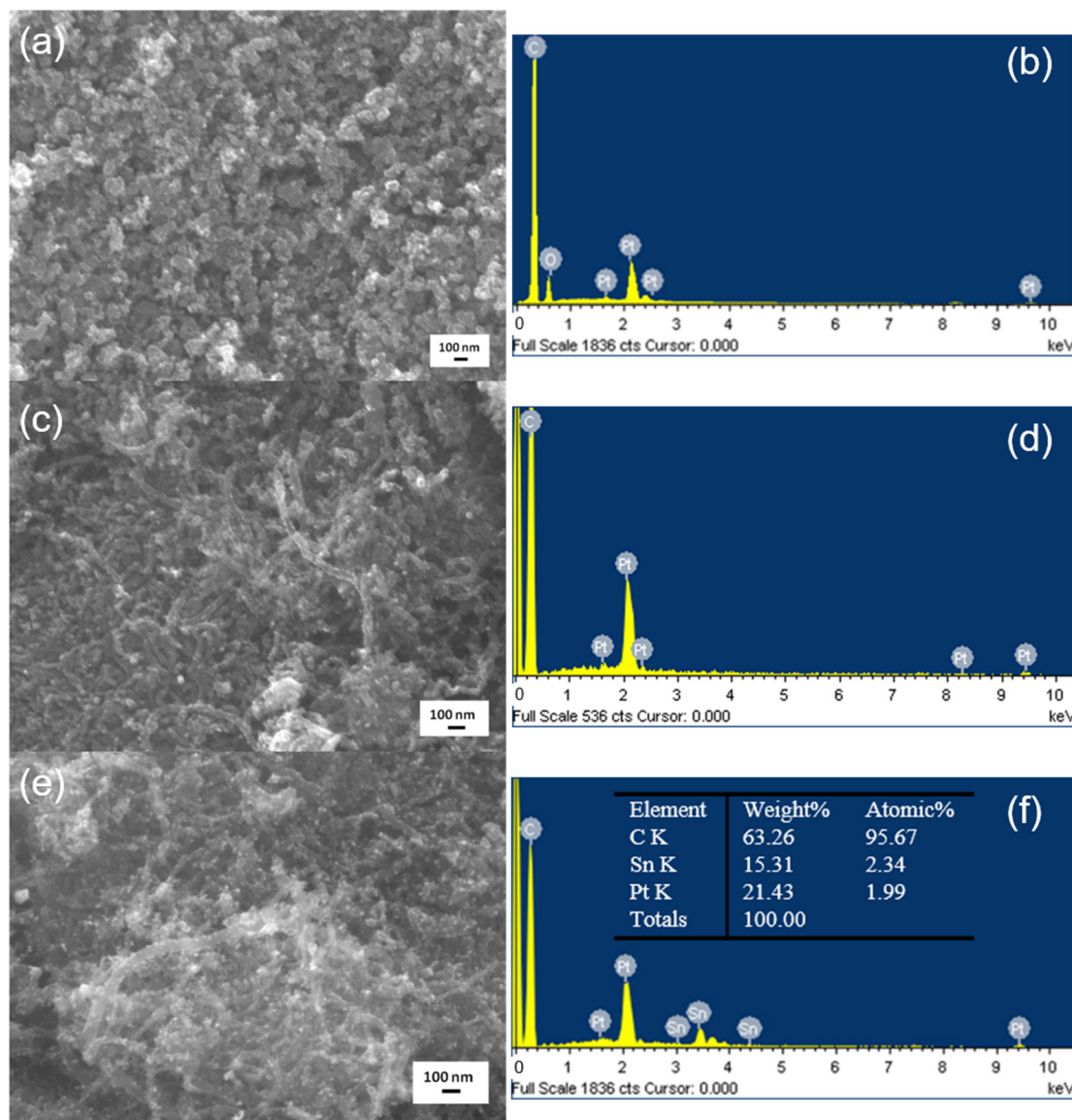


**Figure 5.** Scanning electron microscope (SEM) images and energy dispersive X-ray (EDX) spectra of (a,b) Pt/XC-72; (c,d) Pt/PEI-MWCNTs; and (e,f) PtSn/PEI-MWCNTs.

### 3.4. X-ray Diffraction Analysis

The X-ray diffractograms of various catalysts are shown in Figure 6. The diffraction peaks at  $26.3^\circ$ ,  $43.0^\circ$ ,  $54.3^\circ$ ,  $79.8^\circ$  correspond to the (002), (100), (004), and (110) crystalline planes of the graphite structures of MWCNTs (PDF card 65-6212). The peaks on all three XRD patterns at  $40^\circ$ ,  $47^\circ$ ,  $68^\circ$ ,  $81^\circ$  can be indexed to the (111), (200), (220), and (311) crystalline planes of Pt's face center cubic (fcc) structure [44]. It is noted that the Pt diffraction peaks for PtSn/PEI-MWCNTs are slightly shifted to lower  $2\theta$  angle values with respect to pure Pt (PDF card 4-802). This shift in peak indicates the

formation of PtSn alloy, which is caused by the incorporation of Sn in fcc Pt phase [45,46]. The average size of Pt and PtSn NPs can be calculated using Scherrer equation:

$$d = \frac{0.9\lambda_{K_\alpha}}{B_{2\theta} \cos\theta} \quad (1)$$

where  $d$  is the average particle size (nm),  $\lambda_{K_\alpha}$  is wavelength of X-ray ( $\lambda_{K_\alpha} = 0.15406$  nm),  $\theta$  is angle of Pt (220) peak, and  $B_{2\theta}$  is the full width half maximum in radians [2,46]. The mean particle size of Pt and PtSn NPs are estimated to be 3.1, 2.7, and 4.1 nm for Pt/XC-72, Pt/PEI-MWCNTs and PtSn/PEI-MWCNTs, respectively, which is consistent with TEM observation.

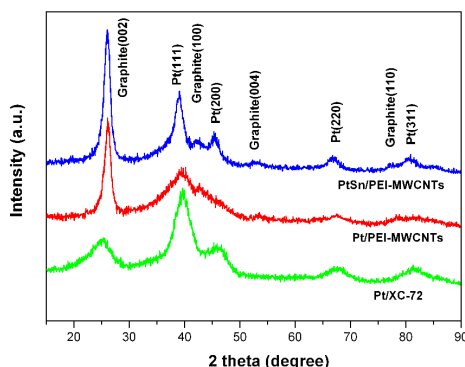


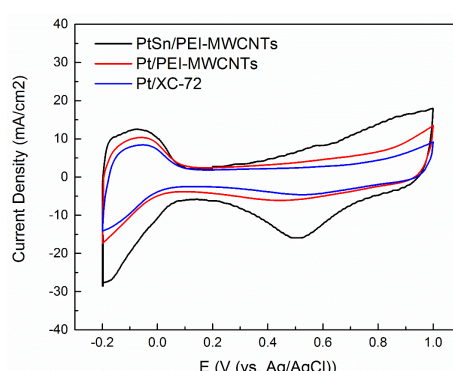
**Figure 6.** X-ray diffraction patterns (XRD) of Pt/XC-72, Pt/PEI-MWCNTs and PtSn/PEI-MWCNTs.

### 3.5. Electrochemical Activity of the Catalysts

The hydrogen electrosorption voltammograms for various electrocatalysts are shown in Figure 7. The characteristic peak in the region of  $-0.2$  V to  $0.1$  V is attributed to atomic hydrogen adsorption on the Pt surface, and the ECSA for the catalysts can be estimated by the following equation:

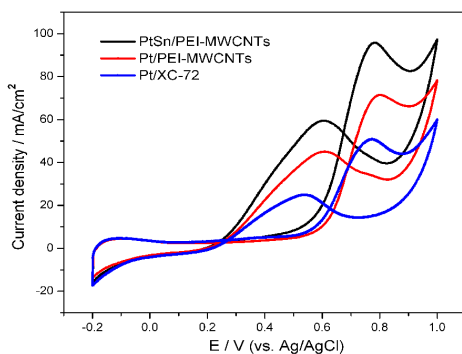
$$\text{ECSA} = \frac{Q}{q^0 \times M_{\text{Pt}}} \quad (2)$$

where  $Q$  is the integrated area of the hydrogen desorption ( $\mu\text{C}$ ),  $q^0$  is the charge for monolayer hydrogen adsorption on Pt,  $q^0 = 210 \text{ C} \cdot \text{cm}^{-2}$ , a value generally admitted for polycrystalline Pt electrodes [47],  $M_{\text{Pt}}$  is the mass of the Pt loading. The PtSn/PEI-MWCNTs catalysts exhibit the largest ECSA, around  $86.6 \text{ m}^2/\text{g}_{\text{Pt}}$ , whereas the Pt/PEI-MWCNTs have a larger ECSA ( $77.7 \text{ m}^2/\text{g}_{\text{Pt}}$ ) than Pt/XC-72 ( $56.2 \text{ m}^2/\text{g}_{\text{Pt}}$ ). These results reveal that non-covalent modification of MWCNTs with PEI facilitate the high dispersion of metal NPs and thus improve the electrochemical performance.



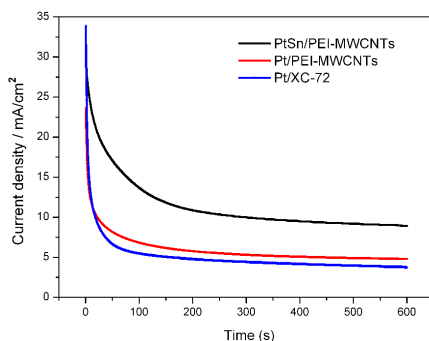
**Figure 7.** Cyclic voltammograms of Pt/XC72, Pt/PEI-MWCNTs and PtSn/PEI-MWCNTs catalysts in  $0.5 \text{ M H}_2\text{SO}_4$  at a scan rate of  $50 \text{ mV/s}$ .

Figure 8 illustrates the CV profiles of ethanol oxidation on various electrocatalysts in 1 M  $\text{C}_2\text{H}_5\text{OH}$  + 0.5 M  $\text{H}_2\text{SO}_4$ . In the forward sweep, the EOR starts at 0.43 V, 0.45 V and 0.35 V for Pt/XC-72, Pt/PEI-MWCNTs and PtSn/PEI-MWCNTs, respectively. The lower onset potential indicates that EOR becomes more energetically favorable on PtSn/PEI-MWCNTs than on the other catalysts [31]. It is also worthwhile to note that the forward peak current densities ( $I_f$ ) experienced in the various materials are ordered as followed, PtSn/PEI-MWCNTs (95.8 mA/cm<sup>2</sup>) > Pt/PEI-MWCNTs (71.4 mA/cm<sup>2</sup>) > Pt/XC-72 (50.8 mA/cm<sup>2</sup>). Compared with Pt/XC-72, the higher  $I_f$  of Pt/PEI-MWCNTs can be elucidated by the fact that more catalyst sites are accessible for electrochemical reactions owing to the larger ECSA. And it is evident that the PtSn/PEI-MWCNTs outperform Pt/PEI-MWCNTs for both EOR and ECSA. Hence, the present of Sn does enhance the catalysis of EOR, which agrees with the reported promoting effect of Sn [44,47].



**Figure 8.** Cyclic voltammograms of Pt/XC72, Pt/PEI-MWCNTs and PtSn/PEI-MWCNTs catalysts in 0.5 M  $\text{H}_2\text{SO}_4$  + 1 M  $\text{C}_2\text{H}_5\text{OH}$  at a scan rate of 50 mV/s.

Figure 9 shows the current-time curves measured at a constant potential 0.6 V in 1 M  $\text{C}_2\text{H}_5\text{OH}$  + 0.5 M  $\text{H}_2\text{SO}_4$ . For all catalysts, the potential-static currents drop rapidly in the initial stage, and then reach a pseudo steady state after a period of approximately 300 s. The initial high current is associated with double-layer charging, while the current decay is caused by the accumulation of poisonous carbonaceous intermediates on the electrode surface [48]. As seen in the chronoamperometric profile, PtSn/PEI-MWCNTs maintain the higher current density and lower current decay rate when compared with Pt/XC-72 and Pt/PEI-MWCNTs. The less pronounced current decline on PtSn/PEI-MWCNTs is indicative of its better poisoning tolerance towards EOR. Based on the bifunctional mechanism, the second metal Sn activates water at lower potentials, which produces adsorbed oxygen-containing species to remove the adsorbed CO and therefore liberate Pt active site. In addition, the ligand effect may also occur to alter the electronic properties of Pt and in turn weaken the Pt–CO bond by introducing Sn element [49,50].



**Figure 9.** Chronoamperograms recorded at 0.6 v vs. Ag/AgCl for ethanol oxidation on Pt/XC72, Pt/PEI-MWCNTs and PtSn/PEI-MWCNTs catalysts in 0.5 M  $\text{H}_2\text{SO}_4$  + 1 M  $\text{C}_2\text{H}_5\text{OH}$ .

#### 4. Conclusions

In summary, Pt and bimetallic PtSn NPs were homogeneously decorated on noncovalent functionalized MWCNTs via in-situ polyol reduction method. This polyelectrolyte modification strategy provided the desirable dispersion of metal NPs on CNTs, and can be extended for the assembly of a large variety of Pt-based hybrid materials. Electrochemical studies demonstrated that the as-synthesized PtSn/PEI-MWCNTs nanocomposites displayed improved catalytic activity towards ethanol electrooxidation with forward current density of  $95.8 \text{ mA/cm}^2$  and a better poisoning tolerance towards as predicted by the bifunctional mechanism. A future study on optimizing the ratio of Pt and Sn in PtSn/PEI-MWCNT catalyst system for further improved performance in DEFC application is desirable.

**Acknowledgments:** No external funding was used in this study. The publication cost in open access was waived by Energies.

**Author Contributions:** Xi Geng and Yinnie Cen contributed equally to this work.

**Conflicts of Interest:** The authors declare no conflict of interest.

#### References

1. Cao, L.; Sun, G.; Li, H.; Xin, Q. Carbon-supported irsn catalysts for direct ethanol fuel cell. *Fuel Cells Bull.* **2007**, *2007*, 12–16. [[CrossRef](#)]
2. Godoi, D.R.M.; Perez, J.; Villullas, H.M. Alloys and oxides on carbon-supported Pt–Sn electrocatalysts for ethanol oxidation. *J. Power Sources* **2010**, *195*, 3394–3401. [[CrossRef](#)]
3. Song, H.; Qiu, X.; Li, F. Promotion of carbon nanotube-supported Pt catalyst for methanol and ethanol electro-oxidation by  $\text{ZrO}_2$  in acidic media. *Appl. Catal. A Gen.* **2009**, *364*, 1–7. [[CrossRef](#)]
4. Kamarudin, M.; Kamarudin, S.; Masdar, M.; Daud, W. Review: Direct ethanol fuel cells. *Int. J. Hydrog. Energy* **2013**, *38*, 9438–9453. [[CrossRef](#)]
5. Badwal, S.; Giddey, S.; Kulkarni, A.; Goel, J.; Basu, S. Direct ethanol fuel cells for transport and stationary applications—A comprehensive review. *Appl. Energy* **2015**, *145*, 80–103. [[CrossRef](#)]
6. Bianchini, C.; Shen, P.K. Palladium-based electrocatalysts for alcohol oxidation in half cells and in direct alcohol fuel cells. *Chem. Rev.* **2009**, *109*, 4183–4206. [[CrossRef](#)] [[PubMed](#)]
7. Jafri, R.I.; Ramaprabhu, S. Multi walled carbon nanotubes based micro direct ethanol fuel cell using printed circuit board technology. *Int. J. Hydrog. Energy* **2010**, *35*, 1339–1346. [[CrossRef](#)]
8. Guo, D.-J.; Qiu, X.-P.; Chen, L.-Q.; Zhu, W.-T. Multi-walled carbon nanotubes modified by sulfated  $\text{Tio}_2$ —A promising support for Pt catalyst in a direct ethanol fuel cell. *Carbon* **2009**, *47*, 1680–1685. [[CrossRef](#)]
9. Gao, G.; Yang, G.; Xu, M.; Wang, C.; Xu, C.; Li, H. Simple synthesis of Pt nanoparticles on noncovalent functional mwnt surfaces: Application in ethanol electrocatalysis. *J. Power Sources* **2007**, *173*, 178–182. [[CrossRef](#)]
10. Pang, H.L.; Lu, J.P.; Chen, J.H.; Huang, C.T.; Liu, B.; Zhang, X.H. Preparation of  $\text{SnO}_2$ -CNTs supported Pt catalysts and their electrocatalytic properties for ethanol oxidation. *Electrochim. Acta* **2009**, *54*, 2610–2615. [[CrossRef](#)]
11. Guha, A.; Lu, W.; Zawodzinski, T.A.; Schiraldi, D.A. Surface-modified carbons as platinum catalyst support for PEM fuel cells. *Carbon* **2007**, *45*, 1506–1517. [[CrossRef](#)]
12. Du, H.; Li, B.; Kang, F.; Fu, R.; Zeng, Y. Carbon aerogel supported Pt–Ru catalysts for using as the anode of direct methanol fuel cells. *Carbon* **2007**, *45*, 429–435. [[CrossRef](#)]
13. Choi, W.C.; Woo, S.I.; Jeon, M.K.; Sohn, J.M.; Kim, M.R.; Jeon, H.J. Platinum nanoclusters studded in the microporous nanowalls of ordered mesoporous carbon. *Adv. Mater.* **2005**, *17*, 446–451. [[CrossRef](#)]
14. Muneendra, P.A.; Santhosh, C.; Grace, A.N. Carbon nanotubes and polyaniline supported Pt nanoparticles for methanol oxidation towards dmfc applications. *Appl. Nanosci.* **2012**, *2*, 457–466. [[CrossRef](#)]
15. Wang, L.; Imura, M.; Yamauchi, Y. Tailored design of architecturally controlled Pt nanoparticles with huge surface areas toward superior unsupported Pt electrocatalysts. *ACS Appl. Mater. Interfaces* **2012**, *4*, 2865–2869. [[CrossRef](#)] [[PubMed](#)]

16. Lee, H.-B.-R.; Baeck, S.H.; Jaramillo, T.F.; Bent, S.F. Growth of Pt nanowires by atomic layer deposition on highly ordered pyrolytic graphite. *Nano Lett.* **2013**, *13*, 457–463. [CrossRef] [PubMed]
17. Kylián, O.; Valeš, V.; Polonskyi, O.; Peščíká, J.; Čechvala, J.; Solař, P.; Choukourov, A.; Slavínská, D.; Biederman, H. Deposition of Pt nanoclusters by means of gas aggregation cluster source. *Mater. Lett.* **2012**, *79*, 229–231. [CrossRef]
18. Li, X.L.; Liu, Y.Q.; Fu, L.; Cao, L.C.; Wei, D.C.; Wang, Y. Efficient synthesis of carbon nanotube–nanoparticle hybrids. *Adv. Funct. Mater.* **2006**, *16*, 2431–2437. [CrossRef]
19. Du, N.; Zhang, H.; Wu, P.; Yu, J.; Yang, D. A general approach for uniform coating of a metal layer on MWCNTs via layer-by-layer assembly. *J. Phys. Chem. C* **2009**, *113*, 17387–17391. [CrossRef]
20. Wang, S.; Jiang, S.P.; Wang, X. Polyelectrolyte functionalized carbon nanotubes as a support for noble metal electrocatalysts and their activity for methanol oxidation. *Nanotechnology* **2008**, *19*. [CrossRef] [PubMed]
21. Li, J.; Yang, W.; Zhu, H.; Wang, X.; Yang, F.; Zhang, B.; Yang, X. *In situ* pei and formic acid directed formation of Pt nps/mwnts hybrid material with excellent electrocatalytic activity. *Talanta* **2009**, *79*, 935–939. [CrossRef] [PubMed]
22. Hu, X.; Wang, T.; Wang, L.; Guo, S.; Dong, S. A general route to prepare one- and three-dimensional carbon nanotube/metal nanoparticle composite nanostructures. *Langmuir* **2007**, *23*, 6352–6357. [CrossRef] [PubMed]
23. Cheng, Y.; Jiang, S.P. Highly effective and co-tolerant PtRu electrocatalysts supported on poly (ethyleneimine) functionalized carbon nanotubes for direct methanol fuel cells. *Electrochim. Acta* **2013**, *99*, 124–132. [CrossRef]
24. Mourdikoudis, S.; Chirea, M.; Altantzis, T.; Pastoriza-Santos, I.; Perez-Juste, J.; Silva, F.; Bals, S.; Liz-Marzan, L.M. Dimethylformamide-mediated synthesis of water-soluble platinum nanodendrites for ethanol oxidation electrocatalysis. *Nanoscale* **2013**, *5*, 4776–4784. [CrossRef] [PubMed]
25. Lamy, C.; Belgsir, E.; Léger, J. Electrocatalytic oxidation of aliphatic alcohols: Application to the direct alcohol fuel cell (dafc). *J. Appl. Electrochem.* **2001**, *31*, 799–809. [CrossRef]
26. Brouzgou, A.; Song, S.; Tsiakaras, P. Low and non-platinum electrocatalysts for pemfcs: Current status, challenges and prospects. *Appl. Catal. B Environ.* **2012**, *127*, 371–388. [CrossRef]
27. Purgato, F.L.S.; Olivi, P.; Léger, J.M.; De Andrade, A.R.; Tremiliosi-Filho, G.; Gonzalez, E.R.; Lamy, C.; Kokoh, K.B. Activity of platinum–tin catalysts prepared by the pechini–adams method for the electrooxidation of ethanol. *J. Electroanal. Chem.* **2009**, *628*, 81–89. [CrossRef]
28. Hitmi, H.; Belgsir, E.M.; Léger, J.M.; Lamy, C.; Lezna, R.O. A kinetic analysis of the electro-oxidation of ethanol at a platinum electrode in acid medium. *Electrochim. Acta* **1994**, *39*, 407–415. [CrossRef]
29. Chen, H.; Tang, Q.; Chen, Y.; Yan, Y.; Zhou, C.; Guo, Z.; Jia, X.; Yang, Y. Microwave-assisted synthesis of PtRu/CNT and PtSn/CNT catalysts and their applications in the aerobic oxidation of benzyl alcohol in base-free aqueous solutions. *Catal. Sci. Technol.* **2013**, *3*, 328–338. [CrossRef]
30. Purgato, F.L.S.; Pronier, S.; Olivi, P.; De Andrade, A.R.; Léger, J.M.; Tremiliosi-Filho, G.; Kokoh, K.B. Direct ethanol fuel cell: Electrochemical performance at 90 °C on Pt and PtSn/C electrocatalysts. *J. Power Sources* **2012**, *198*, 95–99. [CrossRef]
31. Beyhan, S.; Coutanceau, C.; Léger, J.-M.; Napporn, T.W.; Kadırgan, F. Promising anode candidates for direct ethanol fuel cell: Carbon supported PtSn-based trimetallic catalysts prepared by bönnemann method. *Int. J. Hydron. Energy* **2013**, *38*, 6830–6841. [CrossRef]
32. Zhou, W.J.; Song, S.Q.; Li, W.Z.; Zhou, Z.H.; Sun, G.Q.; Xin, Q.; Douvartzides, S.; Tsiakaras, P. Direct ethanol fuel cells based on PtSn anodes: The effect of Sn content on the fuel cell performance. *J. Power Sources* **2005**, *140*, 50–58. [CrossRef]
33. Zhou, W.; Zhou, Z.; Song, S.; Li, W.; Sun, G.; Tsiakaras, P.; Xin, Q. Pt based anode catalysts for direct ethanol fuel cells. *Appl. Catal. B Environ.* **2003**, *46*, 273–285. [CrossRef]
34. Spinacé, E.V.; Linardi, M.; Neto, A.O. Co-catalytic effect of nickel in the electro-oxidation of ethanol on binary Pt–Sn electrocatalysts. *Electrochim. Commun.* **2005**, *7*, 365–369. [CrossRef]
35. Tsiakaras, P. Pt<sub>m</sub>/c (M = Sn, Ru, Pd, W) based anode direct ethanol–pemfcs: Structural characteristics and cell performance. *J. Power Sources* **2007**, *171*, 107–112. [CrossRef]
36. Lee, S.-H.; Ragupathy, D.; Gopalan, A.; Lee, K.-P. Development of novel catalysts by  $\gamma$ -irradiation-induced distribution of Pt–Sn nanoparticles onto multiwalled carbon nanotubes. *J. Nanolectron. Optoelectron.* **2012**, *7*, 444–448. [CrossRef]
37. Jiang, L.; Gao, L. Modified carbon nanotubes: An effective way to selective attachment of gold nanoparticles. *Carbon* **2003**, *41*, 2923–2929. [CrossRef]

38. Dai, J.; Bruening, M.L. Catalytic nanoparticles formed by reduction of metal ions in multilayered polyelectrolyte films. *Nano Lett.* **2002**, *2*, 497–501. [[CrossRef](#)]
39. Wu, H.-X.; Cao, W.-M.; Li, Y.; Liu, G.; Wen, Y.; Yang, H.-F.; Yang, S.-P. *In situ* growth of copper nanoparticles on multiwalled carbon nanotubes and their application as non-enzymatic glucose sensor materials. *Electrochim. Acta* **2010**, *55*, 3734–3740. [[CrossRef](#)]
40. Zou, G.; Yang, H.; Jain, M.; Zhou, H.; Williams, D.; Zhou, M.; McCleskey, T.; Burrell, A.; Jia, Q. Vertical connection of carbon nanotubes to silicon at room temperature using a chemical route. *Carbon* **2009**, *47*, 933–937. [[CrossRef](#)]
41. Jia, N.; Lian, Q.; Shen, H.; Wang, C.; Li, X.; Yang, Z. Intracellular delivery of quantum dots tagged antisense oligodeoxynucleotides by functionalized multiwalled carbon nanotubes. *Nano Lett.* **2007**, *7*, 2976–2980. [[CrossRef](#)] [[PubMed](#)]
42. Bai, L.; Zhu, H.; Thrasher, J.S.; Street, S.C. Synthesis and electrocatalytic activity of photoreduced platinum nanoparticles in a poly(ethylenimine) matrix. *ACS Appl. Mater. Interfaces* **2009**, *1*, 2304–2311. [[CrossRef](#)] [[PubMed](#)]
43. Li, T.; Du, Y.; Wang, E. Polyethyleneimine-functionalized platinum nanoparticles with high electrochemiluminescence activity and their applications to amplified analysis of biomolecules. *Chem. Asian J.* **2008**, *3*, 1942–1948. [[CrossRef](#)] [[PubMed](#)]
44. Li, G.; Pickup, P.G. Decoration of carbon-supported Pt catalysts with Sn to promote electro-oxidation of ethanol. *J. Power Sources* **2007**, *173*, 121–129. [[CrossRef](#)]
45. Zhou, W.J.; Song, S.Q.; Li, W.Z.; Sun, G.Q.; Xin, Q.; Kontou, S.; Poulianitis, K.; Tsakaratas, P. Pt-based anode catalysts for direct ethanol fuel cells. *Solid State Ion.* **2004**, *175*, 797–803. [[CrossRef](#)]
46. Lee, E.; Park, I.-S.; Manthiram, A. Synthesis and characterization of Pt–Sn–Pd/c catalysts for ethanol electro-oxidation reaction. *J. Phys. Chem. C* **2010**, *114*, 10634–10640. [[CrossRef](#)]
47. Tian, N.; Zhou, Z.-Y.; Sun, S.-G.; Ding, Y.; Wang, Z.L. Synthesis of tetrahedral platinum nanocrystals with high-index facets and high electro-oxidation activity. *Science* **2007**, *316*, 732–735. [[CrossRef](#)] [[PubMed](#)]
48. Wang, Z.-B.; Yin, G.-P.; Zhang, J.; Sun, Y.-C.; Shi, P.-F. Investigation of ethanol electrooxidation on a Pt–Ru–Ni/c catalyst for a direct ethanol fuel cell. *J. Power Sources* **2006**, *160*, 37–43. [[CrossRef](#)]
49. Delime, F.; Leger, J.M.; Lamy, C. Enhancement of the electrooxidation of ethanol on a PT–PEM electrode modified by tin. Part I: Half cell study. *J. Appl. Electrochem.* **1999**, *29*, 1249–1254. [[CrossRef](#)]
50. Vigier, F.; Coutanceau, C.; Hahn, F.; Belgsir, E.M.; Lamy, C. On the mechanism of ethanol electro-oxidation on Pt and PtSn catalysts: Electrochemical and *in situ* ir reflectance spectroscopy studies. *J. Electroanal. Chem.* **2004**, *563*, 81–89. [[CrossRef](#)]



© 2016 by the authors; licensee MDPI, Basel, Switzerland. This article is an open access article distributed under the terms and conditions of the Creative Commons by Attribution (CC-BY) license (<http://creativecommons.org/licenses/by/4.0/>).